る。

(3) アイソトープでラベルした被験物質（200μg~1mg/kg）をラットに単回静脈内投与し、一定時間後にラットの各種臓器の放射活性を測定することにより、被験物質の組織分布状況を検討する。

3. 反復投与毒性試験

目的：被験物質を反復投与した時に、明らかな毒性変化を惹起する用量とその変化の内容、及び毒性変化の認められない用量を求める。

方法：少数の動物による用量漸増試験を予備的に実施し、1の安全性薬理試験の結果と総合して反復投与試験における無毒性量および中間量を推定し、雌雄のラットおよびイヌについて4週間の静脈内投与試験を行う。試験計画、観察項目および検査項目はICHおよび厚生労働省のガイドラインに沿って決める。

4. 生殖発生毒性試験

目的：被験物質の哺乳類の生殖発生に対する影響を検討する。

方法：3. の反復投与毒性試験の検討項目の中で、雄生殖器の評価を行う。なお、雄受胎能試験は、大規模臨床試験（第III相試験）の開始前に実施、完了する予定である。なお、今回の臨床研究では妊娠可能な女性を対象としていないので雌受胎能試験は予定していないが、被検物質の一般毒性プロファイルを把握するために、反復投与毒性試験の検討項目として、雌生殖器への影響について詳細に検討する。

5. 遺伝毒性試験

目的：被験物質の変異原性および染色体異常誘発作を検討する。

方法：in vitroで、種々の濃度の被験物質（2μg~2000μg/ml）について、細菌を用いる復帰突然変異試験（Ames試験）、培養細胞或いはヒトリンパ球を用いる染色体異常試験を実施する。

6. 免疫毒性試験

目的：被検物質は生理的な物質ではあるが、高用量を投与するため、免疫毒性の発現の可能性を念のために検討する。

方法：3. の反復投与毒性試験の検討項目の中で、免疫毒性の可能性を示す変化（兆候）（血液学的変化、免疫系器官の変化、血清グロブリン濃度変化等）についての評価を行う。

II. 研究成果の刊行に関する一覧表

発表者氏名	論文タイトル名	発表誌名	巻号	ページ	出版年
Kiyohara E, **Tamai K**, Katayama I, Kaneda Y.	The combination of chemotherapy with HVJ-E containing Rad51 siRNA elicited diverse anti-tumor effects and synergistically suppressedmelanoma.	Gene Ther.	doi: 10.1038/gt.2011.123. [Epub ahead of print]		2011
Nakagami H, Nishikawa T, Tamura N, Maeda A, Hibino H, Mochizuki M, Shimosato T, Moriya T, Morishita R, **Tamai K**, Tomono K, Kaneda Y.	Modification of a novel angiogenic peptide, AG30, for the development of novel therapeutic agents.	J Cell Mol Med.	doi: 10.1111/j.1582-4934.2011.01406.x. [Epub ahead of print]		2011
Tamai K, Yamazaki T, Chino T, Ishii M, Otsuru S, Kikuchi Y, Iinuma S, Saga K, Nimura K, Shimbo T, Umegaki N, Katayama I, Miyazaki J, Takeda J, McGrath JA, Uitto J, Kaneda Y.	PDGFRalpha-positive cells in bone marrow are mobilized by high mobility groupbox 1 (HMGB1) regenerate injured epithelia.	Proc Natl Acad Sci U S A.	108	6609-6614	2011
Hanafusa T, **Tamai K**, Umegaki N, Yamaguchi Y, Fukuda S, Nishikawa Y, Yaegashi N, Okuyama R, McGrath JA, **Katayama I.**	The course of pregnancy and childbirth in three mothers with recessive dystrophic epidermolysis bullosa.	Clin Exp Dermatol	37	10-14	2012

Arase N, Igawa K, Senda S, Terao M, **Murota H**, **Katayama I.**	Morphea on the breast after a needle biopsy.	Ann Dermatol.	23	S408-410	2011
Kotobuki Y, Tanemura A, Yang L, Itoi S, Wataya-Kaneda M, **Murota H**, Fujimoto M, Serada S, Naka T, **Katayama I.**	Dysregulation of melanocyte function by Th17-related cytokines: significance of Th17 cell infiltration in autoimmune vitiligo vulgaris.	Pigment Cell Melanoma Res.	25	219-230	2012
Kitaba S, **Murota H**, Terao M, Azukizawa H, Terabe F, Shima Y, Fujimoto M, Tanaka T, Naka T, Kishimoto T, **Katayama I.**	Blockade of interleukin-6 receptor alleviates disease in mouse model of scleroderma.	Am J Pathol	180	165-176	2012
Wataya-Kaneda M, Tanaka M, Nakamura A, Matsumoto S, **Katayama I.**	A novel application of topical rapamycin formulation, an inhibitor of mTOR, for patients with hypomelanotic macules in tuberous sclerosis complex.	Arch Dermatol.	148	138-139	2012
Wataya-Kaneda M, Tanaka M, Nakamura A, Matsumoto S, **Katayama I.**	A topical combination of rapamycin and tacrolimus for the treatment of angiofibroma due to tuberous sclerosis complex (TSC): a pilot study of nine Japanese patients with TSC of different disease severity	British J Dermatol	165	912-916	2011

Arase N, **Wataya-Kaneda M**, Oiso N, Tanemura A, Kawada A, Suzuki T, **Katayama I**	Repigmentation of leukoderma in a piebald patient associated with a novel c-KIT gene mutation, G592E, of the tyrosine kinase domain.	J Dermatol Sci	64	147-149	2011
Murakami Y, **Wataya-Kaneda M**, Terao M, Azukizawa H, **Murota H**, Nakata Y, **Katayama I**.	Peculiar distribution of tumorous xanthomas in an adult case of erdheim-chester disease complicated by atopic dermatitis.	Case Rep Dermatol.	3	107-112	2011
Hayashi H, Kohno T, Yasui K, **Murota H**, Kimura T, Duncan GS, Nakashima T, Yamamoto K, **Katayama I**, Ma Y, Chua KJ, Suematsu T, Shimokawa I, Akira S, Kubo Y, Mak TW, Matsuyama T.	Characterization of dsRNA-induced pancreatitis model reveals the regulatory role of IFN regulatory factor 2 (Irf2) in trypsinogen5 gene transcription.	Proc Natl Acad Sci U S A.	108	18766-18771	2011
Terao M, **Murota H**, Kimura A, Kato A, Ishikawa A, Igawa K, Miyoshi E, **Katayama I**.	11β-Hydroxysteroid dehydrogenase-1 is a novel regulator of skin homeostasis and a candidate target forpromoting tissue repair.	PLoS One	6	e25039	2011

Terao M, Ishikawa A, Nakahara S, Kimura A, Kato A, Moriwaki K, Kamada Y, **Murota H**, Taniguchi N, **Katayama I**, Miyoshi E.	Enhanced epithelial-mesenchymal transition-like phenotype in N-acetylglucosaminyltransferase V transgenic mouse skin promotes wound healing.	J Biol Chem	286	28303-28311	2011
Terao M, Nishida K, **Murota H**, **Katayama I.**	Clinical effect of tocoretinate on lichen and macular amyloidosis.	J Dermatol.	38	179-184.	2011
Ren LM, Arahira T, Todo M, Yoshikawa H, **Myoui A.**	Biomechanical evaluation of porous bioactive ceramics after implantation: micro CT-based three-dimensional finite element analysis.	J Mater Sci Mater Med.	23	463-472	2011
Kawato Y, Hirao M, Ebina K, Tamai N, Shi K, Hashimoto J, Yoshikawa H, **Myoui A.**	Nkx3.2-induced suppression of Runx2 is a crucial mediator of hypoxia-dependent maintenance of chondrocyte phenotypes.	Biochem Biophys Res Commun.	416	205-210	2011
Tao H, Okamoto M, Nishikawa M, Yoshikawa H, **Myoui A.**	P38 mitogen-activated protein kinase inhibitor, FR167653, inhibits parathyroid hormone related protein-induced osteoclastogenesis and bone resorption.	PLoS One	6	e23199	2011

Yokoi M, Hattori K, Narikawa K, Ohgushi H, Tadokoro M, Hoshi K, Takato T, **Myoui A**, Nanno K, Kato Y, Kanawa M, Sugawara K, Kobo T, Ushida T.	Feasibility and limitations of the round robin test for assessment of in vitro chondrogenesis evaluation protocol in a tissue-engineered medical product.	J Tissue Eng Regen Med.	doi: 10.1002/term.460. [Epub ahead of print]		2011
Shibata M, **Ezoe S**, Oritani K, Matsui K, Tokunaga M, Fujita N, Saito Y, Takahashi T, Hino M, Matsumura I, Kanakura Y.	Predictability of the response to tyrosine kinase inhibitors via in vitro analysis of Bcr-Abl phosphorylation.	Leuk Res.	35	1205- 1211	2011
Fujita J, Mizuki M, Otsuka M, **Ezoe S**, Tanaka H, Satoh Y, Fukushima K, Tokunaga M, Matsumura I, Kanakura Y.	Myeloid neoplasm-related gene abnormalities differentially affect dendritic cell differentiation from murine hematopoietic stem/progenitor	cells.Immunol Lett	136	61-73	2011

III. 研究成果の刊行物・別冊

Gene Therapy (2011), 1–8

www.nature.com/gt

ORIGINAL ARTICLE

The combination of chemotherapy with HVJ-E containing Rad51 siRNA elicited diverse anti-tumor effects and synergistically suppressed melanoma

E Kiyohara[1,2], K Tamai[1,2], I Katayama[2] and Y Kaneda[1]

Dacarbazine (DTIC) is one of the most popular alkylating agents used for the treatment of malignant melanoma. DTIC induces apoptosis of melanoma cells via double-strand breaks (DSBs). Melanoma cells, however, tend to increase their expression of DNA repair molecules in order to be resistant to DTIC. Here, we show that DTIC increases expression of Rad51, but not Ku70, in a cultured B16-F10 mouse melanoma cell line in dose- and time-dependent manners. On introducing Rad51 short interfering RNA (siRNA) with the hemagglutinating virus of Japan envelope (HVJ-E) to B16-F10 cells, DSBs induced by DTIC treatment were not efficiently repaired and resulted in enhanced apoptotic cell death. Colony formation of B16-F10 cells that received Rad51 siRNA was significantly decreased by DTIC treatment as compared with cells that received scramble siRNA. In melanoma-bearing mice, the combination of three intratumoral injections of HVJ-E containing Rad51 siRNA and five intraperitoneal injections of DTIC at a clinical dose synergistically suppressed the tumors. Moreover, HVJ-E demonstrated anti-tumor immunity by inducing cytotoxic T lymphocytes to B16-F10 cells on administration of DTIC. These results suggest that the combination of chemotherapy with HVJ-E containing therapeutic molecules will provide a promising therapeutic strategy for patients bearing malignant tumors resistant to chemotherapeutic agents.
Gene Therapy (2011) **0**, 000–000. doi:10.1038/gt.2011.123

Keywords: HVJ-E; melanoma; immunotherapy; chemotherapy; Rad51

INTRODUCTION

Although a variety of anti-cancer strategies have been developed, chemotherapy remains the first-line treatment for most cancers. However, cancer cells can easily escape from chemotherapy by mutating to become drug resistant, resulting in rather aggressive tumor growth. Dacarbazine (DTIC) is one of the most popular alkylating agents used for the treatment of malignant melanoma. Clinical trials of DTIC with or without other chemical agents, such as tamoxifen and IFN-α, have found that the combination therapies do not result in a significantly prolonged survival period as compared with DTIC alone.[1–3] There is no evidence from randomized controlled clinical trials to show that combination therapy is superior to DTIC alone for the treatment for metastatic cutaneous melanoma.[4] Therefore, it is necessary to enhance the beneficial effects of DTIC for melanoma treatment by overcoming DTIC-induced drug resistance.

Some cancer drugs induce double-strand breaks (DSBs) in tumor DNA. DSBs are immediately repaired by two major nuclear mechanisms: homologous recombination (HR) and non-homologous end joining. The recombinase protein Rad51 is an essential molecule in HR.[5] The core component of non-homologous end joining is a ku70/80 heterodimer, which binds the broken DNA end and recruits DNA-PKcs. Rad51 is overexpressed in a variety of tumors,[6,7] suggesting that Rad51 inhibition may suppress tumor growth by enhancing the effects of DSBs generated by cancer drugs. Previously, we successfully treated HeLa cell tumors in mice by combining cisplatin administration with the suppression of Rad51 mRNA by short interfering RNA (siRNA).[8] We found that the steady-state level of Rad51 expression was elevated in HeLa cells, and that Rad51 knockdown by siRNA induced tumor sensitivity to cisplatin. Another study also showed that the inhibition of Rad51 function increased the sensitivity of doxorubicin to soft tissue sarcoma.[9]

Melanoma cells constitutively express higher levels of Rad51 as compared with normal fibroblasts[10] and have a tendency to become resistant to chemotherapy and radiation, possibly due to Rad51-dependent DSB repair. If DTIC treatment is shown to induce Rad51 expression in melanoma cells, Rad51 knockdown may enhance the DTIC sensitivity of melanomas.

To develop an effective Rad51-knockdown therapy for human cancer patients, highly efficient procedures for *in vivo* siRNA introduction are needed. Recently, we have achieved rather efficient *in vivo* siRNA delivery by using the hemagglutinating virus of Japan envelope (HVJ-E), which is an inactivated Sendai virus particle that was developed as a drug delivery vector.[11–13] Furthermore, HVJ-E itself induces diverse anti-tumor immunity, including dendritic cell maturation, NK cell activation, cytotoxic T lymphocyte (CTL) induction and regulatory T-cell suppression.[14–16] Therefore, therapeutic molecules, such as oligonucleotides, plasmids or siRNA, that are packaged into HVJ-E are expected to have increased anti-cancer activities. Here, we tested the dual synergy of the anti-tumor effects of DTIC treatment combined with Rad51 siRNA-encapsulated HVJ-E. Rad51 siRNA enhanced the cancer-killing activity of DTIC, and anti-tumor immune responses were enhanced by HVJ-E.

[1]Division of Gene Therapy Science, Osaka University Graduate School of Medicine, Osaka, Japan and [2]Department of Dermatology, Graduate School of Medicine, Osaka University, Osaka, Japan
Correspondence: Dr Y Kaneda, Division of Gene Therapy Science, Osaka University Graduate School of Medicine, 2-2 Yamada-oka, Suita, Osaka 565-0871, Japan.
E-mail: kaneday@gts.med.osaka-u.ac.jp
Received 24 January 2011; revised 6 July 2011; accepted 22 July 2011

RESULTS

DTIC treatment increased Rad51 expression in F10 cells

We first examined the effect of DTIC treatment on Rad51 and Ku70 expression in F10 melanoma cells. F10 cells were treated with DTIC for 1 h, and then Rad51 and Ku70 expression was measured. The untreated F10 cells were used as a control. Western blot analysis indicated that Rad51 protein expression increased 1.6-fold at 0 h after stimulation with DTIC, while Ku70 protein expression did not show a significant change (Figures 1a and b). Rad51 and Ku70 expression was measured at various time points after the DTIC was removed (Figures 1c and d). Rad51 expression increased 1.9-fold at 4 h after stimulation with DTIC.

In response to DSBs, histone H2AX is rapidly phosphorylated by ataxia-telangiectasia mutated/ataxia telangiectasia and RAD3 ataxia-telangiectasia mutated related PI3K-family kinases on chromatin to become γ-H2AX.[17–19] Immunofluorescence studies showed that the increased numbers of Rad51 foci were merged with γ-H2AX foci 2 h after 1.1 mM (200 μg ml^{-1}) DTIC treatment (Figure 1e). These two proteins initiate HR complex formation.

Rad51 knockdown prolonged DSBs repair

We then investigated the effect of Rad51 knockdown on the sensitivity of F10 melanoma cells to DTIC. We first checked the Rad51 expression level after introducing Rad51 siRNA by HVJ-E to F10 melanoma cells. Real-time (RT)-PCR analysis indicated that DTIC dosedependently increased Rad51 expression. However, the Rad51 expression caused by DTIC treatment was significantly suppressed by Rad51 siRNA, as compared with scramble siRNA (Figure 2a). In western blot analysis, Rad51 protein expression caused by DTIC treatment was suppressed by Rad51 siRNA, as compared with scramble siRNA (Figure 2b).

Western blot analysis showed that the F10 cells containing Rad51 siRNA had a sustained increase in γ-H2AX caused by DTIC treatment, whereas the level of γ-H2AX in the F10 cells containing scramble siRNA decreased continuously 1 h after DTIC treatment (Figures 2c and d). Immunocytochemistry of γ-H2AX in F10 cells containing Rad51 siRNA showed that the number of γ-H2AX foci in the nuclei increased after DTIC treatment (Figures 3a and b). Quantitative analysis of γ-H2AX foci indicated a five-fold increase at 36 h after the transfer of Rad51 siRNA as compared with scramble siRNA transfer (Figure 3b).

Rad51 knockdown increased the sensitivity of DTIC in F10 cells *in vitro*

To test the effect of Rad51 siRNA and DTIC combination treatment *in vitro*, a colony formation assay and fluorescence-activated cell sorting analysis of annexin V expression were performed. In a colony formation assay of F10 cells after DTIC treatment, the number of colonies of cells transferred with Rad51 siRNA was significantly decreased to 50.2% of the number of colonies of scramble siRNA-transferred cells (Figure 4a).

Rad51 knockdown significantly increased F10 cell apoptosis induced by DTIC. Apoptosis induced by a combination of 0.55 mM (100 μg ml^{-1}) DTIC and Rad51 siRNA was not significantly different from that induced by a combination of 1.1 mM DTIC and scramble siRNA (Figure 4b). Similarly, the combination of 1.1 mM DTIC and Rad51 siRNA showed no significant difference in apoptotic cell number as compared with the combined treatment of 2.2 mM (400 μg ml^{-1}) DTIC and scramble siRNA. These data indicate that the transfer of Rad51 siRNA into F10 cells could induce two-fold greater sensitivities of F10 cells against 0.55 or 1.1 mM DTIC *in vitro*. The combination of DTIC and Rad51 siRNA also increased the sensitivity of B16-F1 mouse melanoma cells to DTIC as seen in B16-F10 cells (Supplementary Figures 1a and b).

HVJ-E enhanced the anti-tumor effect of combined therapy of DTIC with Rad51 siRNA

We then evaluated the anti-tumor activity of HVJ-E, in addition to the DTIC-Rad51 siRNA combination therapy. Three injections of HVJ-E containing Rad51 siRNA into F10 tumors decreased Rad51 protein expression (Figure 5a). Three intratumor injections of phosphate-buffered saline (PBS) or HVJ-E (sc-HVJ: scramble siRNA enclosed by HVJ-E, Rad51-HVJ: Rad51 siRNA enclosed by HVJ-E) combined with five intraperitoneal injections of 80 mg kg^{-1} DTIC were administered when the intracutaneous F10 tumor volume had reached 40 mm^3 on the backs of C57/BL6 mice (Figure 5b). At 29 days post inoculation of F10 cells, sc-HVJ+DTIC and Rad51-HVJ+DTIC resulted in tumor growth inhibition of 41.9% and 77.7%, respectively. Thus, the combination of Rad51 siRNA and DTIC had a greater effect on F10 tumors, as compared with that of scramble siRNA and DTIC. However, even without DTIC significant tumor suppression was observed. On day 29, sc-HVJ+PBS and Rad51-HVJ+PBS resulted in tumor growth inhibition of 31.6% and 29.4%, respectively, as compared with PBS+PBS. These data show that HVJ-E containing siRNA suppresses the growth of F10 tumors *in vivo* irrespective of the variety of siRNA.

HVJ-E induces anti-tumor immunity by various mechanisms. However, it is unknown whether anti-tumor immunity induced by HVJ-E is achieved in the presence of chemotherapy. We examined the immune response induced by HVJ-E *in vivo*. First, the infiltration of $CD4^+$ and $CD8^+$ T cells into tumor tissue was examined. Quantitative RT-PCR analysis also showed that tumors of mice treated with sc-HVJ+PBS and Rad51-HVJ+DTIC had significantly increased $CD8^+$ and $CD4^+$ expression (Figure 5c).

To test the CTL activity induced by HVJ-E, an enzyme-linked immunospot assay was performed (Figure 5d). Lymphocytes from mice treated with sc-HVJ+PBS showed more spots than the control groups, PBS+PBS and PBS+DTIC. Tumors treated with Rad51-HVJ+DTIC also showed the same CTL activity as tumors treated with scHVJ-PBS. Thus, the CTL activity induced by HVJ-E was not inhibited by DTIC. These data indicate that the adaptive immunity activated by HVJ-E was not affected by DTIC treatment and was maintained in the mouse tumor model.

DISCUSSION

In the present study, we demonstrated that the combination chemotherapy of DTIC with Rad51 siRNA delivered by HVJ-E significantly suppressed melanoma *in vitro* and *in vivo*. This novel therapeutic strategy was then shown to elicit both direct apoptosis and anti-tumor immunity, which synergistically suppressed the tumor growth *in vivo*.

Until now, many chemotherapeutic agents have been used alone or in combination to treat melanoma. However, these therapies do not have sufficient efficacies to eradicate melanoma cells, and recurrences are often observed. To overcome these difficulties, it is necessary to increase the sensitivity of tumor cells to chemotherapy or to develop new effective therapies for malignant melanoma. Several approaches have been used to increase the sensitivity of melanoma to DTIC. Intratumor injections of anti-sense oligonucleotides against Clusterin, an anti-apoptotic protein in melanoma cell lines, improved the susceptibility to DTIC.[20] DNA repair molecules are also targets to increase the sensitivity of chemotherapy or radiotherapy. Suppression of ataxia-telangiectasia mutated, ataxia-telangiectasia mutated related

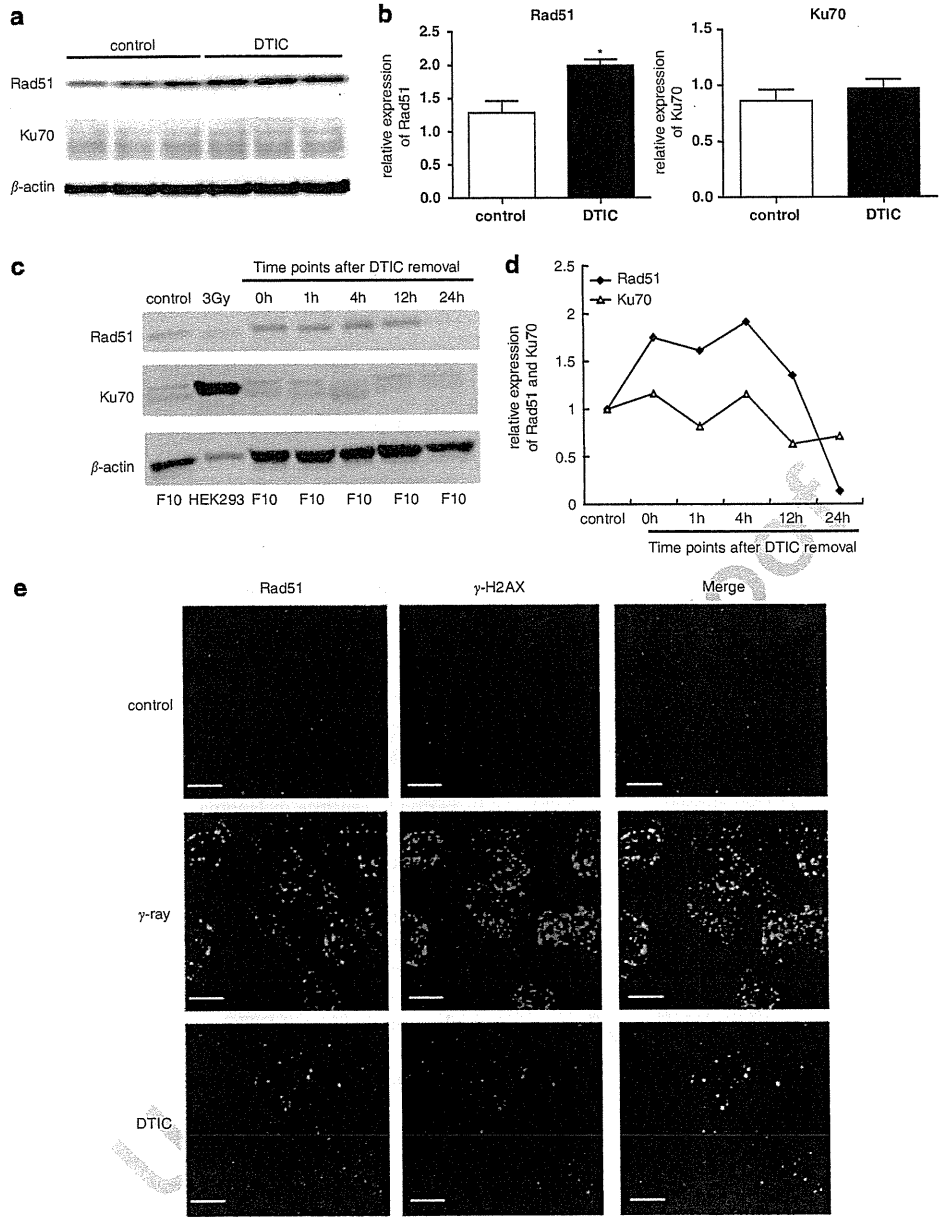

Figure 1 DTIC increased Rad51 protein expression. (**a**) Western blot analysis of Rad51, Ku70 and β-actin levels in F10 cells; 2.2 mM DTIC was added to a culture of F10 cells for 1 h (n=3, each group). (**b**) Statistical analysis of **a.** Rad51 and Ku70 expression was normalized to β-actin expression. Columns are the mean of three samples. Bars, s.d. *$P<0.05$. (**c**) Western blot analysis of Rad51, Ku70 and β-actin levels in F10 cells at the indicated time points after 2.2 mM DTIC treatment. For the positive control, Ku70 and β-actin levels in HEK293 cells were detected 10 min after γ-ray irradiation. (**d**) Quantification of the intensity of Rad51 and Ku70 (in **c**) normalized by β-actin intensity. (**e**) 2.2 mM DTIC was added to cultures of F10 cells for 1 h. Two hours after the DTIC was removed from the cultures, the immunofluorescence of Rad51 and γ-H2AX was determined. For the positive control, F10 cells were examined 10 min after irradiation with 10 Gy γ-ray. Green indicates Rad51 antibody and Alexa Fluor 488-labeled secondary antibody. Red indicates γ-H2AX antibody and Alexa Fluor 546-labeled secondary antibody. Scale bar, 10 μm.

and poly ADP-ribose polymerase inhibits the initiation of DNA repair and enhances apoptosis in combination with chemotherapy.[21,22]

Among DNA repair molecules, Rad51 plays a main role in DSB repair in the HR pathway. Cancer cells have been targeted by their tendency to highly express Rad51. A Rad51 promoter-driven diphtheria toxin A gene efficiently induced apoptosis when introduced into cancer cells.[23] Gefitinib, an epidermal growth-factor receptor inhibitor, reduced the Rad51 expression induced by cisplatin or mitomycin C by blocking ERK1/2 activation.[24] Under the suppression of Rad51 by gefitinib, human lung cancer cells became more sensitive to chemotherapeutic agents. Rad51 expression was also shown to be increased by fusion of tyrosine kinase BCR/Abl in chronic myelogenous leukemia.[25] Gleevec, an agent that inhibits c-Abl expression, inhibits the BCR/Abl fusion gene expression in tumor cells to decrease

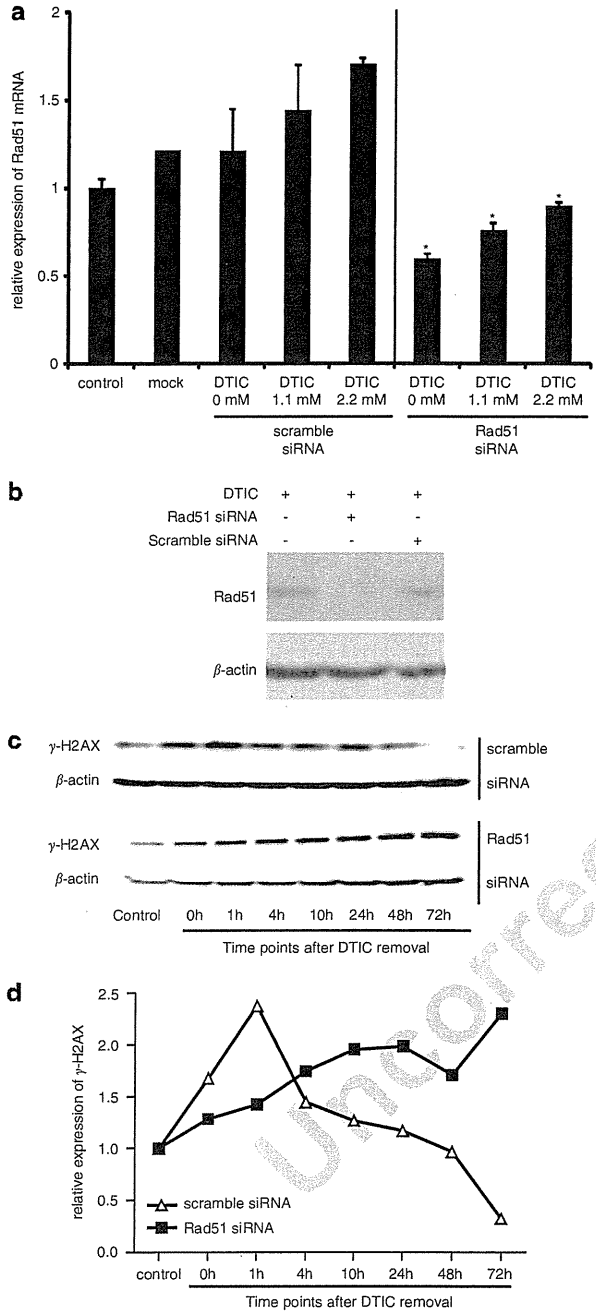

Figure 2 Rad51 mRNA and protein were suppressed by Rad51 siRNA introduced by HVJ-E. The following assays were performed 24 h after the HVJ-E-mediated transfer of Rad51 siRNA or scramble siRNA into F10 cells. (**a**) RT-PCR analysis of Rad51 mRNA, 1 h after the removal of DTIC. Cells were treated with DTIC for 1 h. Rad51 expression was normalized to glyceraldehyde-3-phosphate dehydrogenase expression. Columns, mean of three independent experiments; bars, s.d. $*P<0.05$, Rad51 siRNA columns versus representative scramble siRNA columns. (**b**) F10 melanoma cells were treated with 1.1 mM DTIC for 1 h. Then, 1 h after the removal of DTIC, Rad51 and β-actin were analyzed by western blot. (**c**) Western blot analysis of γ-H2AX and β-actin expression at the indicated times after the removal of 2.2 mM DTIC treatment. The 0-h time point is just after the removal of DTIC. (**d**) Quantification of γ-H2AX normalized to β-actin in **c**.

Rad 51 expression and enhance the radiosensitivity of tumor cells.[26] For these reasons, Rad51 is an attractive target to increase the sensitivity of anti-cancer drugs.

Here, we showed that DTIC treatment increased Rad51 expression in mouse melanoma cells, and that the combination of DTIC with Rad51 siRNA treatment induced the collaborative suppression of mouse melanoma cell growth.

DTIC produces O^6-methylguanine as a focus to generate DSBs. Temozolomide is one of the alkylating agents that increase O^6-methylguanine-mediated DSBs. Knockout of XRCC2, a member of the Rad51 complex, sensitizes tumor cells to temozolomide.[27] Taken together, these findings suggest that Rad51-mediated HR is a common repair mechanism of O^6-methylguanine-mediated DSBs. Following DSBs, repair proteins, such as meiotic recombination 11 and replication protein A, recruit Rad51 to form a complex on the site of DSBs.[28] The Rad51-mediated HR pathway functions in the S and G2 phases owing to requirement of the homologous template, whereas Ku-mediated non-homologous end joining functions mainly in the G1 phase.[29] A previous study showed that DTIC caused cell-cycle arrest and DSBs in the S and G2 phases in mouse melanoma cell lines.[30] In human colon cancer HCT116 cells, DSBs caused by camptothecin were coordinately repaired by cell cycle checkpoint-induced G2 arrest and rapid activation of Rad51-mediated HR.[31] In this report, increased Rad51 expression was shown to reflect DSBs generated by camptothecin in the cancer cells, and was maintained for 6 h after removal of camptothecin stimulation. Our study also showed prolonged elevation of Rad51 expression after removal of DTIC. These findings suggest that Rad51-mediated HR may take several hours to repair DSBs, and Rad51 siRNA treatment must target during this period to sensitize melanoma cells to DTIC by DSB-induced apoptosis.

In the present study, we observed synergistic effects when DTIC treatment was combined with Rad51 siRNA, but not with sc-siRNA, by evaluating the enhancement factor (EF), which is used for evaluating the synergistic effects of combination therapy.[32] If the EF is two-fold greater than the control, the combination effect is defined as synergistic. The EF of the combination of DTIC with Rad51 siRNA was 3 against the combination of DTIC with PBS, whereas the EF of the combination of DTIC with sc-siRNA was 1 against the combination of DTIC with PBS. These data indicate that Rad51 siRNA introduced by HVJ-E synergistically suppressed F10 tumor growth with DTIC treatment *in vivo*.

HVJ-E itself further enhances the anti-cancer effect of DTIC chemotherapy combined with Rad51 siRNA by inducing anti-tumor immunity. We previously reported that the intratumoral administration of Rad51 siRNA by HVJ-E enhanced the anti-tumor effect of cisplatin against HeLa cell growth in severe combined immunodeficiency mice without immune responses.[8] However, we showed here that the efficient induction of CTL activity against tumor cells with infiltrating effector lymphocytes was evident in F10 cell tumors in C57/BL6 mice if treated with HVJ-E, regardless of its contents. Therefore, the scHVJ-PBS group showed some anti-tumor activity by the induction of CTL against melanoma cells. The mechanism of HVJ-E-mediated anti-tumor immunity involves the activation and inactivation of various immune cells, as described in Introduction. Previous chemo-immunotherapies, such as the combination of DTIC with interferon-alfa-2b or interleukin-2, enhanced the anti-cancer efficacy as compared with DTIC alone. However, those chemo-immunotherapies failed to significantly improve the survival of advanced-stage melanoma patients.[33] The present study is the first report to show that the intratumoral administration of Rad51 siRNA by HVJ-E would further enhance the chemo-immunotherapeutic

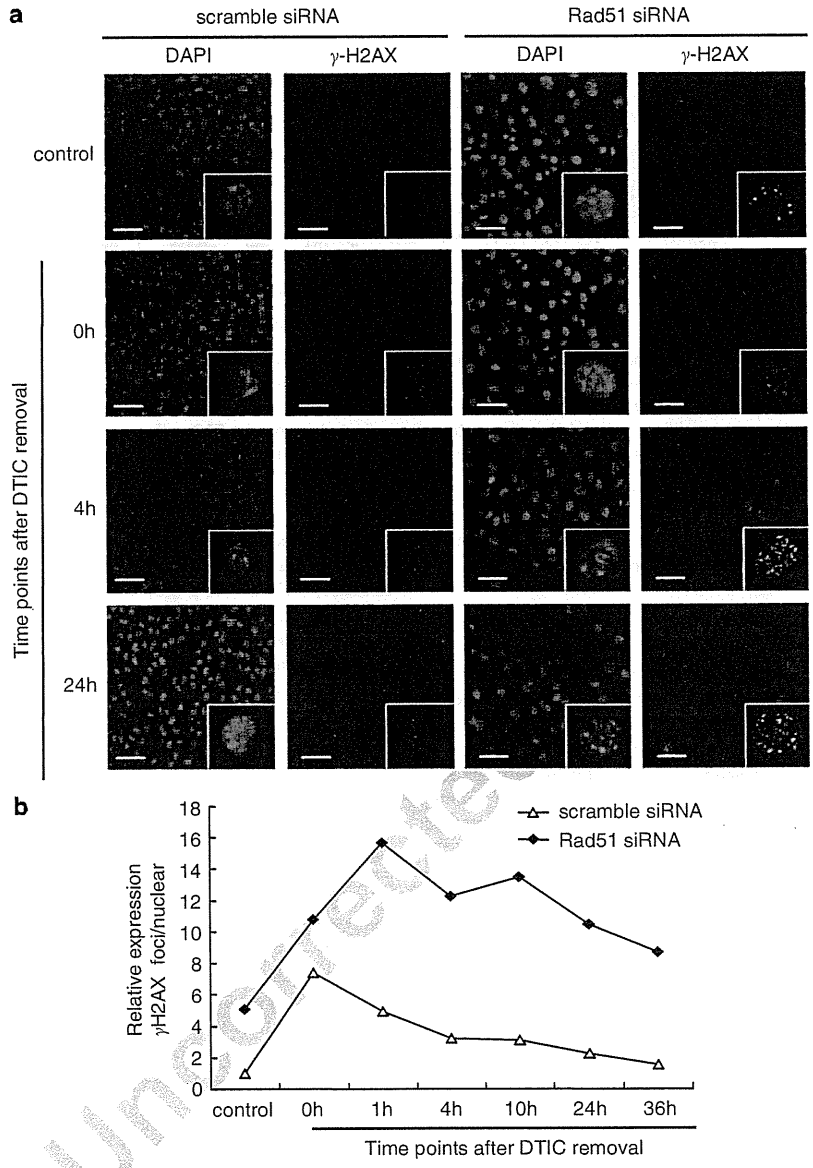

Figure 3 DSBs caused by DTIC treatment were not repaired after Rad51 siRNA induction. (**a**) Immunofluorescence of γ-H2AX foci at the indicated times after a 1-h treatment with 1.1 mM DTIC. The 0-h time point is just after the removal of DTIC from the medium. The fixed cells were stained by γ-H2AX antibody and Alexa Fluor 488-labeled secondary antibody. Nuclei were stained by 4′,6-diamino-2-phenylindole. Scale bar, 100 μm. (**b**) Relative γ-H2AX levels were calculated as the ratio of γ-H2AX foci to the number of nuclei.

activity of DTIC with HVJ-E-mediated CTL activity against melanoma cells *in vivo*.

To obtain sustained CTL activity induced by HVJ-E, DTIC chemotherapy itself may exert adverse effects due to myeloablative conditioning. Because the combination treatment of DTIC with Rad51 siRNA could reduce the necessary dose of DTIC by half, this combination therapy seems to have multiple advantages not only to overcome DTIC resistance due to Rad51 induction, but also to optimize the DTIC dosage to maintain CTL activity by HVJ-E.

Although further precise analysis is necessary to optimize the chemo-immunotherapy composed of DTIC, Rad51 siRNA-encapsulated HVJ-E may be an ideal therapeutic strategy, because the remaining tumor cells after DTIC treatment would be eliminated by HVJ-E-induced anti-cancer immunity. Thus, this novel therapeutic strategy may provide a future perspective to overcome the difficulties underlying current therapies for malignant melanoma. Furthermore, a similar strategy of combined chemo-immunotherapy may be applied to other intractable malignant tumors with less sensitivity to current chemotherapy protocols.

In summary, Rad51 siRNA treatment synergistically enhanced the anti-melanoma activity of DTIC *in vivo*. HVJ-E, which delivered Rad51 siRNA to melanoma cells, further enhanced the therapeutic effect by inducing anti-tumor immunity. Thus, we showed dual synergy of the anti-tumor effects of Rad51 siRNA-encapsulated HVJ-E in combination with DTIC treatment. Such a combination of chemotherapy with HVJ-E containing therapeutic molecules will

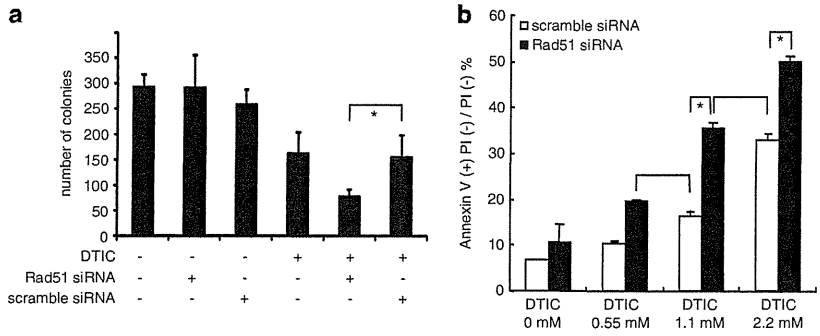

Figure 4 Rad51 siRNA induced higher susceptibility of F10 cells against DTIC treatment. (a) 1×10^5 F10 cells transferred with HVJ-E vector-mediated siRNA (scramble or Rad51) were cultured for 24 h. The cells were treated with 1.1 mM DTIC. Twenty-four hours later, the treated cells were seeded at a density of 500 cells per dish. After 7 days, the colonies were counted. Columns indicate the mean of three independent experiments; bars, s.d. $*P<0.05$. (b) Annexin V (+) propidium iodide (−)/propidium iodide (−) in flow cytometry indicated apoptosis. F10 cells, after receiving siRNA by HVJ-E, were treated with the indicated concentrations of DTIC. White columns indicate scramble siRNA and black columns indicate Rad51 siRNA. Columns are the mean of three independent experiments. Bars, s.d. $*P<0.05$.

provide a promising therapeutic approach for patients suffering from intractable cancer, such as malignant melanoma.

MATERIALS AND METHODS

Chemicals and cell lines

DTIC was purchased from Kyowa Hakko Co. (Tokyo, Japan). The S9-cofactor set was purchased from Oriental Yeast Co., Ltd (Tokyo, Japan). The S9 mixture was prepared by adding one volume of cofactor solution ($MgCl_2$, KCl, glucose-6-phosphate, NADPH and NADH in sodium phosphate buffer, pH 7.4) as described previously.[34] The mouse melanoma B16-F10 cells, B16-F1 cells and human HEK293 cells were purchased from the American Tissue Culture Collection, which tested the cells for viability and lack of contamination. F10 cells were grown in Dulbecco's modified Eagle's medium supplemented with 10% fetal bovine serum and 5% penicillin-streptomycin. HEK293 cells were grown in minimum essential medium supplemented with 10% fetal bovine serum and 5% penicillin-streptomycin. F10 cells and HEK293 cells were incubated at 37 °C in a humidified atmosphere with 5% CO_2.

HVJ-E preparation and siRNA transfection

HVJ in suspension was inactivated by UV irradiation (99 $mJcm^{-2}$). The inactivated HVJ suspension (HVJ-E) was centrifuged at 18 500 *g* for 15 min at 4 °C. Then, the supernatant was removed, and the HVJ-E was suspended in PBS at 4 °C. Rad51 siRNA (5′-GCAGCGAUGUCCUAGAUAA-3′) solution (Dharmacon) was mixed with 5 µl of 5 $mg\,ml^{-1}$ protamine sulfate (Nakalai Tesque, Tokyo, Japan) for 5 min. Scrambled siRNA (5′-UGGUUUACAUGUCG ACUAA-3′) solution (Dharmacon) was mixed with 5 µl of 5 $mg\,ml^{-1}$ protamine sulfate (Nakalai Tesque) for 5 min and was used as a control. HVJ-E was mixed with siRNA solution and Triton X-100 (final concentration, 0.2%) for 5 min. After centrifugation (18 500 *g* for 15 min at 4 °C), the supernatant was removed and HVJ-E that contained siRNA was suspended in PBS.

Western blot

The harvested cancer cells were suspended in lysis buffer, as previously described.[35] An equal amount of sample buffer was mixed with the cell lysates, and the samples were boiled for 5 min and vortexed twice. Each cell lysate was electrophoresed on a 12% sodium dodecyl sulfate polyacrylamide gel and transferred onto a 0.45-µm polyvinylidene fluoride membrane (Millipore, Bedford, MA, USA). The membrane was blocked with 5% skim milk and probed with a primary antibody: mouse anti-Rad51 (×100, Spring Bioscience), mouse anti-β-actin (×5000, Sigma), mouse anti-Ku70 (×200, Abcam, UK) or mouse anti-γ-H2AX ×200, Millipore). The membranes were washed and labeled with horseradish peroxidase–conjugated anti-mouse whole IgG (×1000, Amersham Biosciences, Uppsala, Sweden) and goat anti-rabbit IgG (×1000, Amersham Biosciences) antibodies at room temperature for 1 h. Detection by chemiluminescence was performed following the standard protocol provided by the manufacturer (Amersham, Buckinghamshire, UK). Western bands were edited by Photoshop software (Adobe). Semiquantification of Rad51, γ-H2AX and β-actin was performed by densitometric analysis with Scion Image software. Blots were calculated in order by clicking special, loading Macros, opening Macros, selecting Gelplot2, opening image files, selecting the band area of images, opening Mark First Lane, opening Plot Lanes3, selecting the area and selecting the result.

Immunocytochemistry

Drug-treated cells were fixed with 4% paraformaldehyde for 10 min, permeabilized for 10 min with 0.1% Triton X-100, and blocked with 5% goat serum for 1 h at room temperature. The slides were incubated for 1 h with primary antibodies, mouse anti-Rad51 (×100, Spring Bioscience) or rabbit anti-mouse γ-H2AX (×200, Calbiochem, Frankfurter, Germany). Nuclei were stained with 4′,6-diamino-2-phenylindole. The slides were incubated for 1 h with secondary antibodies conjugated to goat anti-mouse IgG Alexa 488 or goat anti-rabbit IgG Alexa 546 (×500, Molecular Probes). Cells were analyzed by using a Radiance 2100 laser scanning confocal microscope system (Bio-Rad) equipped with an inverted Nikon Eclipse TE-2000 microscope (Nikon, Tokyo, Japan) and Plan-Apo objective lens (Nikon). The contrast of all images was adjusted by Photoshop software (Adobe). The γ-H2AX count was determined with Image J.

Quantitative RT-PCR

For *in vitro* assays, 2 µg of total RNA extracted from tumors was reverse transcribed into cDNA by a high-capacity cDNA reverse transcription kit (Applied Biosystems, Foster City, CA, USA) and amplified by real-time quantitative RT-PCR with an ABI PRISM 7900HT Sequence Detection system (Applied Biosystems) under the following conditions: 40 cycles of denaturation at 94 °C for 45 s, annealing at 49 °C for 45 s and elongation at 68 °C for 2 min. For *in vivo* analysis, Isogen (Nippon Gene, Japan) was used to extract total RNA from tumors that had been resected and washed in PBS. A sum of 2 µg of the total RNA was reverse transcribed into cDNA and analyzed as *in vitro*. Probes and primer pairs specific for murine Rad51, $CD8^+$, $CD4^+$, and glyceraldehyde-3-phosphate dehydrogenase were purchased from Applied Biosystems. The concentration of target genes was determined by using the comparative threshold cycle method (threshold cycle number at the cross-point between amplification plot and threshold), and values were normalized to an internal glyceraldehyde-3-phosphate dehydrogenase control.

Colony formation assay

F10 cells (1×10^5) were cultured in six-well plates. Twenty-four hours after 300 HAU HVJ-E vector-mediated 200 pmol siRNA transfection per well, the cells were treated with 1.1 mM DTIC. Twenty-four hours later, the treated cells were seeded in a 10-cm dish at a density of 500 cells per dish. After 7 days, the

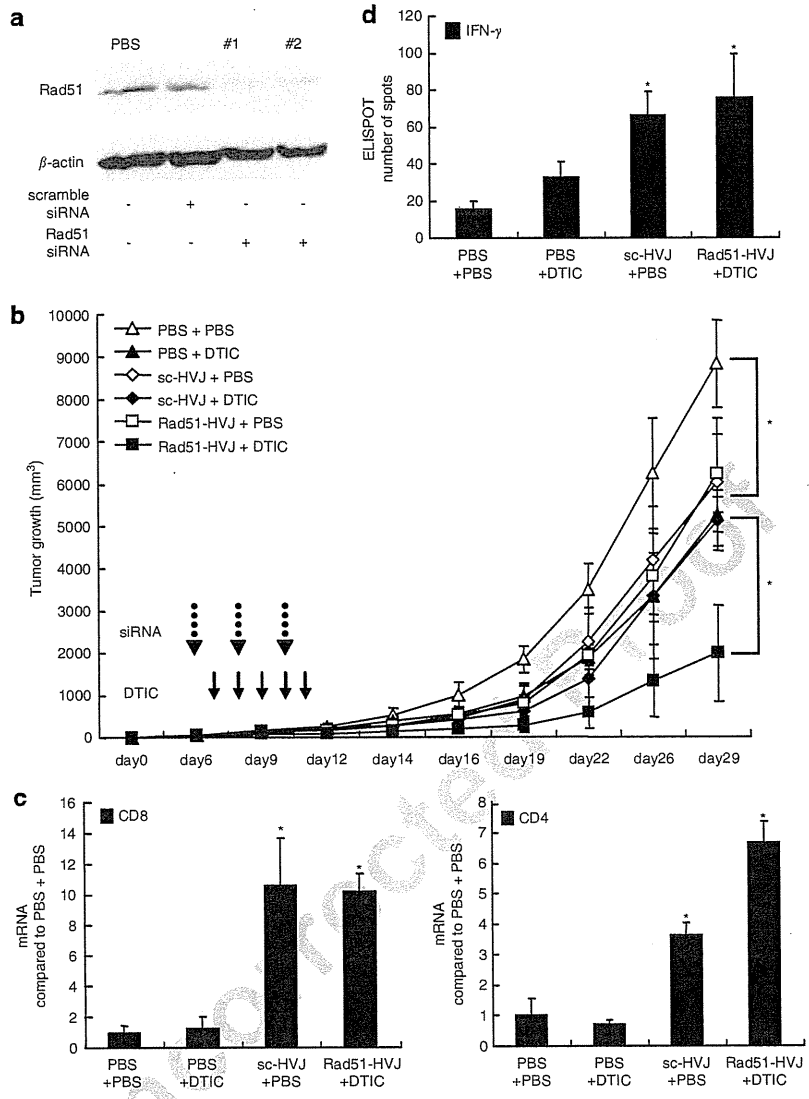

Figure 5 The combination of Rad51 siRNA enclosed by HVJ-E and DTIC synergistically suppressed the growth of F10 tumors. (**a**) Western blot analysis of Rad51 and β-actin expression in F10 tumors transferred with siRNA enclosed by HVJ-E. C57 BL/6 mice were challenged with 5×10^5 F10 cells by subcutaneous injection on the dorsal surface. After the tumors reached 40 mm^3, 1.5×10^3 HAU HVJ-E enclosing 2.5 nmol siRNA or PBS was injected into the tumors on three successive days. The tumors were removed 24 h after the third injection of siRNA. Rad51 expression levels of two tumors (no. 1 and no. 2) injected with Rad51 siRNA were 15.7% and 16.3%, respectively, compared with PBS. (**b**) Tumor growth inhibition assay. C57 BL/6 mice (n=5, each group) were challenged with 5×10^5 F10 cells by subcutaneous injection on the dorsal surface. After the tumor size reached 40 mm^3, 1.5×10^3 HAU HVJ-E enclosing 2.5 nmol siRNA or PBS was injected into the tumors once every other day on days 6, 8 and 10. DTIC (80 mg/kg) dissolved in 100 μl of PBS or 100 μl of PBS was intraperitoneally injected into the mice once every day from day 7 to 11. sc-HVJ: scramble siRNA enclosed by HVJ-E, Rad51-HVJ: Rad51 siRNA enclosed by HVJ-E. Bars, s.d. *P<0.05. (**c**) Quantitative RT-PCR analysis in F10 tumors. The tumors were removed from the mice 48 h after the last intraperitoneal injection of DTIC or PBS in **b** (n=3). Bars, s.d. *P<0.05. (**d**) Enzyme-linked Immunospot assay of IFN-γ from lymphocytes collected from the spleen 7 days after the last intraperitoneal injection of DTIC or PBS in **b** (n=3). Bars, s.d. *P<0.05.

colonies were fixed with methanol, stained with trypan blue (Nacalai Tesque, Tokyo, Japan), and counted.

Annexin V staining

F10 cells (1×10^5 per well) were cultured in six-well plates. Twenty-four hours after transfer of 200 pmol siRNA by 300 HAU HVJ-E per well, the cells were treated with 0.55, 1.1 or 2.2 mM DTIC. Twenty-four hours later, the treated cells were washed twice with PBS and re-suspended in labeling solution. A total of 5 μl of annexin V and 5 μl of propidium iodide (Becton Dickinson PharMingen) were added to the re-suspended solution. After incubation in the dark for 20 min at room temperature, the stained cells were analyzed with a fluorescence-activated cell sorting flow cytometer (Becton Dickinson) and Cell Quest software (Becton Dickinson). Q9 Q10

In vivo experiment

Female 5- to 6-week-old C57 BL/6 mice (purchased from the Jackson Laboratory, ~~M~~I, USA) were challenged with 5×10^5 F10 cells by subcutaneous injection on the dorsal surface. After tumors reached 40 mm^3, 1.5×10^3 HAU Q11

HVJ-E enclosing 2.5 nmol siRNA in 100 μl PBS or PBS was injected into the tumors. DTIC (80 mg kg^{-1}) dissolved in 100 μl of PBS or 100 μl of PBS was intraperitoneally injected into the mice. Tumor volume was measured by the following formula: tumor volume (mm^3)=length×(width)^2/2.

Enzyme-linked immunospot assay

The mice were killed 7 days after the fifth intraperitoneal injection. Splenocytes were harvested from the spleen and cultured as in the previous study.[15] A total of 1×10^4 lymphocytes were cultured with 0.2×10^4 mitomycin C-treated F10 cells at 37 °C for 24 h. The assay was performed by using a mouse IFN-γ enzyme-linked immunospot kit (R&D Systems). The number of spots was subsequently counted under a dissecting microscope (Leica, Cambridge, UK).

EF analysis

The EF was calculated by dividing the normalized tumor growth delay by the absolute growth delay.[33] Absolute growth delay was defined as the time, in days, for tumors to reach 1967 mm^3 (the average tumor size of the combination group treated with Rad51-HVJ and DTIC at 29 days) in the treated group minus the mean time to reach 1967 mm^3 in the untreated control group (PBS). The normalized tumor growth delay was defined as the time, in days, for tumors to reach 1967 mm^3 in mice treated by the combination treatment minus the time, in days, for tumors to reach 1967 mm^3 in the group treated with DTIC alone.

Statistical analysis

In vitro results were analyzed with the Student's non-paired *t*-test. *Post hoc* multiple comparisons of *in vivo* results were made by using Tukey's test. Differences with *P*-values <0.05 were considered statistically significant.

CONFLICT OF INTEREST

The authors declare no conflict of interest.

ACKNOWLEDGEMENTS

This work was supported by the Northern Osaka (Saito) Biomedical Knowledge-Based Cluster Creation Project, Scientific Research (B) Fund by the Ministry of Education, Culture, Sports, Science and Technology of Japan and grants from the Ministry of Health, Labor, and Welfare of Japan.

1 Atkins MB, Buzaid AC, Houghton AN. Systemic chemotherapy and biochemotherapy. In: Balch CM *et al.* (eds). *Cutaneous Melanoma*, 4th edn. Quality Medical Publishing: St Louis, 2003, pp 589–604.
2 Chapman PB, Einhorn LH, Meyers ML, Saxman S, Destro AN, Panageas KS *et al.* Phase III multicenter randomized trial of the Dartmouth regimen versus dacarbazine in patients with metastatic melanoma. *J Clin Oncol* 1999; **17**: 2745–2751.
3 Huncharek M, Caubet JF, McGarry R. Single-agent DTIC versus combination chemotherapy with or without immunotherapy in metastatic melanoma: a meta-analysis of 3273 patients from 20 randomized trials. *Melanoma Res* 2001; **11**: 75–81.
4 Tom C, Reg F, Bernadette C, Malcolm M. Systemic treatments for metastatic cutaneous melanoma. *Cochrane Database Syst Rev* 2000; **2**: CD001215.
5 Peter B, Stephen CW. Role of the human RAD51 protein in homologous recombination and double-stranded-break repair. *Trends Biochem Sci* 1998; **23**: 247–251.
6 Maacke H, Jost K, Opitz S, Miska S, Yuan Y, Hasselbach L *et al.* DNA repair and recombination factor Rad51 is over-expressed in human pancreatic adenocarcinoma. *Oncogene* 2000; **19**: 2791–2795.
7 John T. The Rad51 gene family, genetic instability and cancer. *Cancer Lett* 2005; **219**: 125–135.
8 Makoto I, Seiji Y, Keisuke N, Kazuya H, Hiraoka K, Tamai K *et al.* Rad51 siRNA delivered by HVJ envelope vector enhances the anti-cancer effect of cisplatin. *J Gene Med* 2005; **7**: 1044–1052.
9 Jonathan AFH, Juehui L, Zhu QS, Bolshakov SV, Li L, Pisters PW *et al.* Rad51 overexpression contributes to chemoresistance in human soft tissue sarcoma cells: a role for p53/activator protein 2 transcriptional regulation. *Mol Cancer Ther* 2007; **6**: 1651–1659.
10 Elke R, Karen S, Susanne F, Vanessa S, Schweiger S, Haaf T *et al.* Elevated levels of Rad51 recombination protein in tumor cells. *Cancer Res* 2002; **62**: 219–225.
11 Kondo Y, Fushikida K, Fujieda T, Sakai K, Miyata K, Kato F *et al.* Efficient delivery of antibody into living cells using a novel HVJ envelope vector system. *J Immunol Meth* 2008; **332**: 10–17.
12 Kaneda Y, Nakajima T, Nishikawa T, Yamamoto S, Ikegami H, Suzuki N *et al.* Hemagglutinating virus of Japan (HVJ) envelope vector as a versatile gene delivery system. *Mol Ther* 2002; **6**: 219–226.
13 Takami Y, Nakagami H, Morishita R, Katsuya T, Cui TX, Ichikawa T *et al.* Ubiquitin carboxy-terminal hydrolase L1, a novel deubiquitinating enzyme in the vasculature, attenuates NF-κB activation. *Arterioscler Thromb Vasc Biol* 2007; **27**: 2184–2190.
14 Kurooka M, Kaneda Y. Inactivated Sendai virus particles eradicate tumors by inducing immune responses through blocking regulatory T cells. *Cancer Res* 2007; **67**: 227–236.
15 Fujuhara A, Kurooka M, Miki T, Kaneda Y. Intratumoral injection of inactivated Sendai virus particles elicits strong antitumor activity by enhancing local CXCL10 expression and systemic NK cell activation. *Cancer Immunol Immunother* 2008; **57**: 73–84.
16 Matsuda M, Yamamoto T, Matsumura A, Kaneda Y. Highly efficient eradication of intracranial glioblastoma using Eg5 siRNA combined with HVJ envelope. *Gene Therapy* 2009; **16**: 1465–1476.
17 Emmy PR, Duane RP, Ann HO, Ivanova VS, Bonner WM. DNA double-strand breaks induce histone H2AX phosphorylation on serine 139. *J Biol Chem* 1998; **273**: 5858–5868.
18 Thomas S, Sarah AW, Karen C, Goodarzi AA, Petermann E, Concannon P *et al.* ATR-dependent phosphorylation and activation of ATM in response to UV treatment or replication fork stalling. *EMBO* 2006; **25**: 5775–5782.
19 Ashby JM, Xuetong S. DNA repair in the context of chromatin. *Cell Cycle* 2005; **4**: 568–571.
20 Christoph H, Barbara P, Christiane T, Winter D, Fink D, Kovacic B *et al.* Clusterin regulates drug-resistance in melanoma cells. *J Invest Dermatol* 2005; **124**: 1300–1307.
21 Emma B, Derek JR, Bin-Bing SZ, Kum KK. Recent advances in cancer therapy targeting proteins involved in DNA double-strand break repair. *Clin Cancer Res* 2009; **15**: 6314–6320.
22 Nicola JC. PARP inhibitors for cancer therapy. *Expert Rev Mol Med* 2005; **15**: 603–617.
23 Christopher MH, Andrei S, Vera G. Use of the Rad51 promoter for targeted anti-cancer therapy. *Proc Natl Acad Sci USA* 2008; **105**: 20810–20815.
24 Jen-Chung K, Shih-Ci C, Chau-Ming C, Wang LH, Hong JH, Jheng MY *et al.* Involvement of Rad51 in cytotoxicity induced by epidermal growth factor receptor inhibitor (gefitinib, IressaR) and chemotherapeutic agents in human lung cancer cells. *Carcinogenesis* 2008; **29**: 1448–1458.
25 Artur S, Christoph S, Gregory T, Nieborowska-Skorska M, Hoser G, Nowicki MO *et al.* BCR/ABL regulates mammalian RecA homologs, resulting in drug resistance. *Mol Cell* 2001; **8**: 795–806.
26 Jeffery SR, Kristin B, William EB, Cerra MA, Oswaid KA, Camphausen K *et al.* Gleevec-mediated inhibition of Rad51 expression and enhancement of tumor cell radiosensitivity. *Cancer Res* 2003; **63**: 7377–7383.
27 Roman T, kerstin F, John T, Kaina B. Xrcc2 deficiency sensitizes cells to apoptosis by MNNG and the alkylating anticancer drugs temozolomide, fotemustine and mafosfamide. *Cancer Lett* 2006; **239**: 305–313.
28 Bolderson E, Richard DJ, Zhou BBS, Khanna KK. Recent advances in cancer therapy targeting proteins involved in DNA double-strand break repair. *Clin Cancer Res* 2009; **15**: 6314–6320.
29 Eric W, David JC. The endless tale of non-homologous end-joining. *Cell Res* 2008; **18**: 114–124.
30 Olszewska-Slonina DM, Styczynisk J, Drewa TA, Olszewski KJ, Czajkowski R. B16 and cloudman S91 mouse melanoma cells susceptibility to apoptosis after dacarbazine treatment. *Acta Pol Pharm* 2005; **62**: 473–483.
31 Min H, Ze-Hong M, Hong Z, Yu-Jun C, Wei L, Jian D. Chk1 and Chk2 are differentially involved in homologous recombination repair and cell cycle arrest in response to DNA double-strand breaks induced by camptothecins. *Mol Cancer Ther* 2008; **7**: 1440–1449.
32 Kim J, Kim PH, Yoo JY, Yoon AR, Choi HJ, Seong J *et al.* Double E1B 19kDa- and E1B 55 kDa-deleted oncolytic adenovirus in combination with radiotherapy elicits an enhanced anti-tumor effect. *Gene Therapy* 2009; **16**: 1111–1121.
33 Atkins MB, Hsu J, Lee S, Cohen GI, Flaherty LE, Sosman JA *et al.* Phase III trial comparing concurrent biochemotherapy with cisplatin, vinblastine, dacarbazine, interleukin-2, and interferon alfa-2b with cisplatin, vinblastine, and dacarbazine alone in patients with metastatic malignant melanoma (E3695): a trial coordinated by the Eastern Cooperative Oncology Group. *J Clin Oncol* 2008; **26**: 5748–5754.
34 Masayuki S, Masumi H, Yasumitsu T, Takano TY, Nakatsu Y, Tsuzuki T *et al.* Modes of actions of two types of anti-neoplastic drugs, dacarbazine and ACNU, to induce apoptosis. *Carcinogenesis* 2007; **28**: 2657–2663.
35 Saga K, Tamai K, Kawachi M, Shimbo T, Fujita H, Yamazaki T *et al.* Functional modification of Sendai virus by siRNA. *J Biotechnol* 2008; **133**: 386–394.

Supplementary Information accompanies the paper on Gene Therapy website (http://www.nature.com/gt)

J. Cell. Mol. Med. Vol XX, No X, 2011 pp. 1-11

Modification of a novel angiogenic peptide, ag30, for the development of novel therapeutic agents

Hironori Nakagami [a, b, *], Tomoyuki Nishikawa [a], Nao Tamura [c], Akito Maeda [d], Hajime Hibino [e], Masayoshi Mochizuki [e], Takashi Shimosato [f], Toshinori Moriya [f], Ryuichi Morishita [g], Katsuto Tamai [a], Kazunori Tomono [h], Yasufumi Kaneda [a, *]

[a] *Division of Gene Therapy Science, Osaka University Graduate School of Medicine, Osaka, Japan*
[b] *Division of Vascular Medicine and Epigenetics, Osaka University United Graduate School of Child Development, 2-1 Yamada-oka, Suita, Osaka 565-0871, Japan*
[c] *Anges-MG, Inc. 7-7-15 Saito Bio-Incubator, Ibaraki, Osaka, Japan*
[d] *Skin Regeneration, PIAS Collaborative Research, The Center for Advanced Science and Innovation, Osaka University, Osaka, Japan*
[e] *Peptide Institute, Inc. 7-7-15 Saito Asagi, Ibaraki, Osaka, Japan*
[f] *Research Department, NISSEI BILIS Co. Ltd., Koka, Shiga, Japan*
[g] *Department of Clinical Gene Therapy, Osaka University Graduate School of Medicine, Osaka, Japan*
Q1 [h] *Division of Infection Control and Prevention, Graduate School of Medicine, Suita, Osaka, Japan*

Received: February 12, 2011; Accepted: July 28, 2011

Abstract

We previously identified a novel angiogenic peptide, AG30, with antibacterial effects that could serve as a foundation molecule for the design of wound-healing drugs. Toward clinical application, in this study we have developed a modified version of the AG30 peptide characterized by improved antibacterial and angiogenic action, thus establishing a lead compound for a feasibility study. Because AG30 has an α-helix structure with a number of hydrophobic and cationic amino acids, we designed a modified AG30 peptide by replacing several of the amino acids. The replacement of cationic amino acids (yielding a new molecule, AG30/5C), but not hydrophobic amino acids, increased both the angiogenic and the antimicrobial properties of the peptide. AG30/5C was also effective against *methicillin-resistant Staphylococcus aureus* (MRSA) and antibiotic-resistant *Pseudomonas aeruginosa.* In a diabetic mouse wound-healing model, the topical application of AG30/5C accelerated wound healing with increased angiogenesis and attenuated MRSA infection. To facilitate the eventual clinical investigation/application of these compounds, we developed a large-scale procedure for the synthesis of AG30/5C that employed the conventional solution method and met Good Manufacturing Practice guidelines. In the evaluation of stability of this peptide in saline solution, RP-HPLC analysis revealed that AG30/5C was fairly stable under 5°C for 12 months. Therefore, we propose the use of AG30/5C as a wound-healing drug with antibacterial and angiogenic actions.

Keyword: angiogenesis • antimicrobial • translational research • drug development

Introduction

Antimicrobial peptides are small proteins that are used by the innate immune system to combat bacterial infections in multicellular eukaryotes. The emergence of drug-resistant bacteria has driven the extensive investigation of these peptides as a potential source of new antimicrobial drugs that could complement current antibiotic regimes [1, 2]. In general, antimicrobial peptides are characterized by a net positive charge and an amphipathic three-dimensional structure that gives the peptides an electrostatic affinity to the outer leaflet of the microbial membrane, mediated by lipid molecules on bacterial surfaces [3]. This affinity leads to binding, disruption of the membrane and microbial cell death [4]. More than 100 antimicrobial peptides have been discovered in animals ranging from insects to humans; however, the development of antimicrobial peptide-based

*Correspondence to: Hironori NAKAGAMI, M.D., Ph.D.,
Yasufumi KANEDA, M.D., Ph.D.,
Division of Gene Therapy Science,
Graduate School of Medicine, Osaka University,
2-2 Yamada-oka, Suita 565–0871, Japan.
Tel.: +81-6-6879-3901
Fax: +81-6-6879-3909
E-mail: nakagami@gts.med.osaka-u.ac.jp, kaneday@gts.med.osaka-u.ac.jp

doi:10.1111/j.1582-4934.2011.01406.x

therapies has mainly been restricted to topical or local treatments because their activity is suppressed in serum [3–5].

We recently developed a novel antimicrobial peptide, named AG30, with angiogenic properties potentially similar to those of LL37 or PR39 [6]. Because both angiogenic and antimicrobial effects are beneficial in the process of wound healing, we initiated the clinical development process using AG30 as a foundation compound to develop novel topically applied wound-healing drugs. The development of a peptide-drug based topical treatment has several attractive features: (1) the drug is delivered directly to the wound; (2) high local tissue levels can be achieved through application of aggressive doses; and (3) the short half life of peptides, resulting from their degradation by peptidases, reduces their toxicity. Historically, similar cationic antimicrobial peptides, such as pexiganan, iseganan and omiganan, failed to pass the phase II or III trials in topical applications or systemic applications. Therefore, in this study, we developed the load compound based on a feasibility study using the foundation compound, AG30. Using both *in silico* and functional analyses, we produced a modified version of the AG30 peptide that may elicit more potent angiogenic and antimicrobial effects. As initial steps in the investigation of the potential clinical applications of this modified AG30 peptide, we developed a cost-effective production process and evaluated its efficiency using animal models.

Material and methods

Cell migration assay and tube formation assays and cell growth assay

Human aortic endothelial cells (HAEC, passage 3) were purchased from Clonetics Corp. (Palo Alto, CA, USA) and maintained in endothelial basal medium (EBM-2) that was supplemented with 5% foetal bovine serum (FBS) and endothelial growth supplement as described previously [6]. Cells were incubated at 37°C in a humidified atmosphere of 95% air–5% CO_2 with exchange of medium every 2 days.

Human aortic endothelial cells migration was assayed using a modified Boyden chamber, as previously described [7]. Human aortic endothelial cells tube formation assays were conducted in triplicate in 24-well plates using an Angiogenesis Kit (Kurabo, Osaka, Japan) according to the manufacturer's instructions, as previously described [6].

Human epidermal keratinocytes cell line (HaCaT cells) were maintained with DMEM supplemented with 10% FBS and 10 μg/ml Gentamicin. We used the MTS [3-(4,5-dimethylthiazol-2-yl)-5-(3-carboxymethoxyphenyl)-2-(4-sulfophenyl)-2H- tetrazolium] assay for cell growth. Second day after stimulation with AG30/5C, 10 μl of Cell Riter 96 One Solution Reagent (Progema, Medison, WI, USA) was added to each well, and absorbance at 490 nm was measured [6].

Peptide design and synthesis and circular dichroism (CD) spectroscopy analysis

All peptides used in this experiment were purchased from the Peptide Institute, Inc. (Osaka, Japan). LL37 was synthesized as described previously [8]. The Boman Index was used to predict the function of the peptides [9]. We used the AGADIR program (http://www.embl-heidelberg.de/ExternalInfo/serrano/agadir/agadir-start.html) to predict the structure. Circular dichroism data were acquired with a Jasco J-820 spectrophotometer using a 1-mm-path-length cuvette at 20°C [10]. Spectra were collected for samples containing 0.3 μg/ml peptide in 20 mM phosphate buffer at pH 7.5, with and without the addition of 30% or 60% trifluoroethanol (TFE) [11].

Measurement of MICs against *P. aeruginosa*, *S. Aureus* and *Candida*

The minimum inhibitory concentrations (MICs, expressed as μg/ml) of modified AG30 and LL37 for *Psudomonas aeruginosa* (*P. aeruginosa*, ATCC27853), *Staphylolcoccus aureus* (*S. aureus*, ATCC29213) and *Candida albicans* (*Candida*, ATCC90028) and *methicillin-resistant S. aureus* (MRSA) were defined as the lowest concentration of peptide that inhibited visible bacterial growth after incubation for 16 hrs at 37°C with vigorous shaking, as previously described [6]. This experimental protocol was approved by the bio-safety committee at the Osaka University Graduate School of Medicine.

Mouse wound model and infection models

In the mice tail wound model, full-thickness wounds were made on the dorsal surface of mouse tails as previously described [12]. For wound-healing model, 9-week-old male C57BL/6 db/db mice were used in this study. We completely removed hair from the backs of mice using fine-tooth clippers and hair-removing cream 3 days prior to operation. After induction of anaesthesia, 15 mm punch biopsy wounds were made on the backs of each mouse (n = 10–12 in each group). After topical application of each peptide (100 μg/ml), the wounds were covered with a semi-permeable polyurethane dressing. Topical application of each peptide and measurements of wound areas were repeated on days 0, 2, 4, 7, 9, 11, 14 and 16. Samples were obtained 7 days after the operation. After fixation in cold acetone (at −20°C for 15 min.), capillary EC were identified by immunohistochemical staining using an antimouse PECAM mAb (Pharmingen, San Diego, CA, USA) and then counted in 10 independent views of each group [13]. After day 16, peptide application and film dressing were halted for 10 days, and hair growth was observed.

Similar to the mouse wound model, we made wounds on the backs of db/db mice (n = 6–8 in each group). We topically applied 100 μl of methicillin-resistant *S. aureus* on the wounds (1×10^4 cfu/ml) with or without each peptide tested (100 μg/ml). The wounds were then covered with a semi-permeable polyurethane dressing. Topical application of each peptide and measurements of wound areas by taking pictures were repeated on days 0, 2, 4, 7, 9, 11, 14 and 16. All animal experiments were performed according to the Guidelines for Animal Experiments at the Osaka University Graduate School of Medicine.

Measurement of blood flow by Lase Doppler imaging

Measurement of blood flow with Laser Doppler imaging (LDI; Moor Instruments, Axminister, UK) was performed as described previously [13,

14]. Because Laser Doppler flow velocity correlates with capillary density, we measured the blood flow just below the skin by LDI. Consecutive measurements were obtained over the same regions of interest by averaging four sites around the wound.

Porcine wound-healing model

In the porcine wound model, full-thickness wounds were made on the side abdomen surface of pigs as modified previous method [15]. Three male NIBS minipigs (32.0, 32.1 or 33.5 kg) were used (NARC Corporation, Chiba). Pigs were pre-medicated with ketamine (500 mg/body) and isoflurane (2–4%) were administered for anaesthesia. We completely removed hair from the side abdomen of pigs using fine-tooth clippers and outlined the circle in a 25 mm diameter. Full-thickness excisional wounds were created in a uniform depth of 10 mm. We created four wounds on one side at intervals of 30 mm. After topical application (200 μl/site) of each peptide (100 μg/ml), the wounds were covered with a semipermeable polyurethane dressing. Topical application of each peptide was repeated on days 0, 2, 4, 6, 8 and 10. Samples were obtained 12 days after the operation. These frozen sections were stained with haematoxylin and eosin for overall morphological observation. After fixation in cold acetone (at −20°C for 15 min.), capillary EC were identified by immunohistochemical staining with von Willebrand factor (1:200 dilution; DAKO) [16]. All animal experiments were performed according to the Guidelines for Animal Experiments at the Osaka University Graduate School of Medicine.

Statistical analysis

All values are expressed as means ± S.E.M. Analysis of variance with subsequent Fisher's PLSD test analysis was used to determine the significance of differences in multiple comparisons.

Results

Development of a modified versions of the AG30 peptide

We previously identified a novel angiogenic peptide consisting of 30 amino acids, named AG30 [6]. As shown in Figure 1A, AG30 is a good foundation molecule for the development of wound-healing drugs, and this study may help to establish the feasibility of AG30-related lead compounds for clinical applications. The original AG30 molecule has an amphipathic structure; most of the positively charged amino acids are localized to one side of the molecule, while most of the hydrophobic amino acids are localized to the opposite side [6]. Notably, AG30 contains very few proline or glycine residues that would interrupt the α-helical structure. Thus, in our design strategy for developing modified AG30 molecules, we replaced several neutral amino acids (specifically proline, asparagine, asparagine acid and serine) with cationic or hydrophobic amino acids and added a capping structure (Ac-KLT on the C-terminus and KGI-amido on the N-terminus) to stabilize the helical structure [15] (Fig. 1B). The total net charge of each designed peptide is increased by adding cationic amino acids (AG30: +11, AG30/2C: +14, AG30/5C: +17, respectively).

We evaluated the potential activity of these candidate peptides using two different types of *in silico* analysis. To predict the structure, we used the AGADIR program, an algorithm based on the helix/coil transition theory that predicts the helical behaviour of monomeric peptides [17, 18]. In this analysis, the addition of five hydrophobic amino acids and a capping structure increased the score, although the addition of two or five cationic amino acids decreased the score (Fig. 1C). The Boman Index [9] was used to predict the function of the peptides; this index is calculated by adding the free energies of the side chains for transfer from cyclohexane to water and dividing that sum by the total number of residues. In this analysis, the addition of cationic amino acids gave a high score, while the addition of hydrophobic amino acids and a capping structure decreased the score (Fig. 1C).

Evaluation of modified AG30 peptides

As an initial evaluation of the designed peptides, we investigated their effects on the migration and tube forming ability of human aortic endothelial cells. In the migration assay, the addition of five cationic amino acids (*i.e.* compound AG30/5C) resulted in increased migration activity; however, the addition of a capping structure (*i.e.* compound AG30+Cap) resulted in a lower activity compared to AG30 (Fig. 1D). In the tube formation assay, the addition of cationic charged or hydrophobic amino acids strongly induced tube formation. However, the addition of a capping structure reduced this activity (Fig. 1E and F). We also examined the antibacterial effects of the designed peptides against *P. aeruginosa*, *Candida* and *S. aureus*. The addition of two or five cationic amino acids (*i.e.* compound AG30/2C or AG30/5C) increased the antibacterial activity against all bacteria, although the addition of five hydrophobic amino acids (*i.e.* compound AG30/5H) resulted in a lower antibacterial activity than AG30 (Fig. 2A–D). These results suggest that the addition of five cationic amino acids (*i.e.* compound AG30/5C) enhances both the angiogenic and the antimicrobial properties of the original AG30 molecule, a result that is compatible with the previously determined Boman Index scores.

In the structural analysis of the peptides using CD spectroscopy, all of the candidate peptides showed negligible helical structure in aqueous buffer; the addition of the helix-inducing cosolvent TFE (either 20% or 60%) resulted in the appearance of a clear helical component. This was demonstrated by the minimums at 208 and 220 nm and the increase of ellipticity at 200 nm, which resulted in the appearance of a clear helical component in all of the generated peptide. But the control peptide did not change upon the addition of TFE. We quantified the helical structure [19] formation tendency of each of the peptides, either with or without TFE (Fig. 3A–F). Unexpectedly, the addition of either five

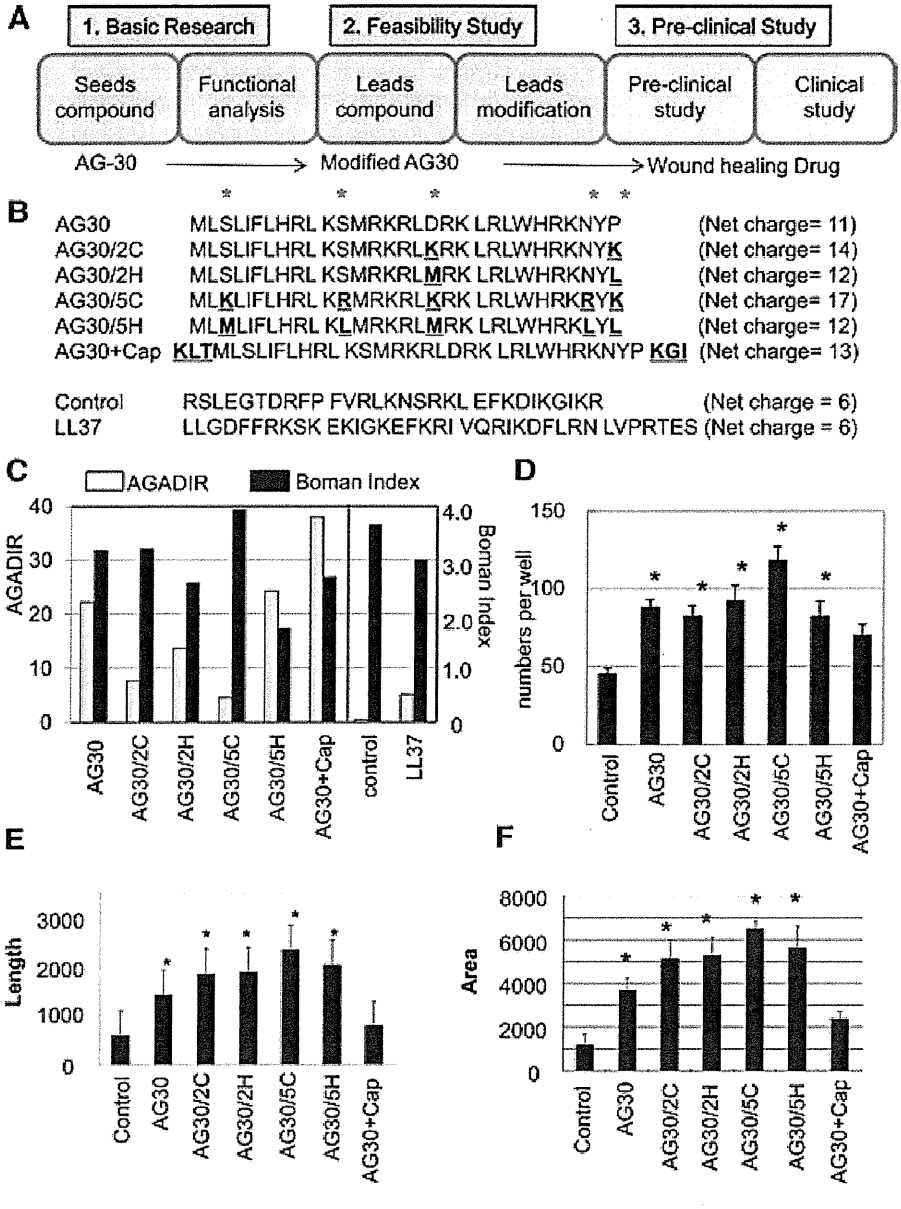

Fig. 1 Several different modified AG30 peptides were created by replacing hydrophobic or cationic amino acids or adding capping structures. (**A**) Study design of this research. AG30 can be a good seed for wound-healing drug and this modified AG30 may correspond to be lead compounds as feasibility study toward clinical application (towards wound-healing drug). (**B**) Peptide sequences and net charge of modified AG30, control peptide and LL37. '*' indicates positions where amino acids were replaced. 'AG30/2C' and 'AG30/5C' indicate the replacement of two or five cationic amino acid (from S, S, D, N, P to K, R, K, R, K, respectively). 'AG30/2H' and 'AG30/5H' indicate the replacement of two or five hydrophobic amino acids (from S, S, D, N, P to M, L, M, L, L, respectively). 'AG30+Cap' indicates the addition of a capping structure (Ac-KLT on the C-terminus and KGI-amide on the N-terminus). (**C**) *In silico* analysis of modified AG30. AGADIR (white bar) scores were calculated to predict the peptide structure and the Boman Index (black bar) was calculated to predict the pleiotropic effects of cationic peptides. (**D**) HAEC migration after treatment with modified AG30 for 24 hrs. (**E**, **F**) Tube formation after daily treatment with modified AG30 for 4 days; length and area were measured. $N = 6$ per group and duplicated. $^{*}P < 0.05$ *vs.* control, $^{\dagger}P < 0.05$ *vs.* AG30.

hydrophobic amino acids (*i.e.* compound AG30/5H) or a capping structure (*i.e.* compound AG30+Cap) did not increase the ratio of α-helical structures, and the addition of five cationic amino acids (*i.e.* compound AG30/5C) decreased the α-helical structure ratio in comparison to AG30. These results suggest that the ratio of α-helical structures upon the addition of TFE does not correspond to the AGADIR score and thus might not correspond to the angiogenic or antibacterial properties of each peptide. Similarly, the well-known antimicrobial peptide LL37 has a low AGADIR score but was found to possess an α-helical structure without addition of TFE. Furthermore, LL-37 has strong angiogenic effects and a high Boman Index score, indicating that the Boman index is more reliable for *in silico* screening in our study.

Antibacterial effects of modified AG30 (AG30/5C)

The advantage of using antimicrobial peptides as antibacterial agents is that bacteria are less likely to become resistant to these compounds in comparison to antibiotics. Indeed, the antibacterial effects (MICs) of AG30 and AG30/5C against MRSA were similar to their effects against methicillin-sensitive *S. aureus* (Fig. 2C and D).

Thus, we examined the MICs of AG30 and AG30/5C against antibiotic-resistant strains (A–E) of *P. aeruginosa* that were resistant to several types of antibiotics. Notably, AG30 and AG30/5C were both effective against antibiotic-resistant *P. aeruginosa* (Table 1). In this assay, AG30/5C also showed a more powerful antibacterial effect in comparison to the original AG30 peptide. Its